B_{1g} RAMAN SCATTERING THROUGH A QUANTUM CRITICAL POINT*

J.K. Freericks

Department of Physics, Georgetown University
Washington, DC 20057, USA

T.P. Devereaux

Department of Physics, University of Waterloo, Canada

and R. Bulla

Theoretische Physik III, Elektronische Korrelationen und Magnetismus
Institut für Physik, Universität Augsburg
D-86135 Augsburg, Germany

(Received June 21, 2001)

A wide variety of strongly correlated insulators ranging from intermediate valence materials, to Kondo insulators, to underdoped high-temperature superconductors display anomalous behavior in their inelastic light scattering. The Raman response in these materials shows a low-temperature transfer of spectral weight from low to high energy (as T is reduced), the appearance of an isosbestic point (a characteristic frequency where the Raman response is independent of temperature), and a large ratio of twice the "spectral gap" to the "onset temperature" where the low-energy spectral weight begins to deplete. We illustrate how these features generically appear in the Raman response of model systems that are tuned to lie just on the insulating side of the metal–insulator transition. We solve for the Raman response in the Falicov–Kimball model and in the Hubbard model. In the latter case, we find a number of new features arise as one approaches the metal–insulator transition from the metallic Fermi-liquid phase. Such behavior has not yet been seen in experiment.

PACS numbers: 78.30.–j, 71.30.+h, 74.72.–h, 75.20.Hr

* Presented at the XII School of Modern Physics on Phase Transitions and Critical Phenomena, Lądek Zdrój, Poland, June 21–24, 2001.

1. Introduction

Raman scattering involves the inelastic scattering of light by the electronic and phononic excitations of a material. Use of polarizers on the incident light and on the reflected light allows one to select elementary excitations of a given symmetry. One of the most common choices is crossed polarizers, which yield B_{1g} symmetry, that has a d-wave character to it. Recent work has focused on *electronic* Raman scattering as an important tool in extracting information about the charge excitations of correlated materials. Remarkably, one finds that a wide variety of materials, ranging from mixed-valence compounds [1] (such as SmB_6), to Kondo-insulators [2] (such as FeSi), to underdoped cuprate high temperature superconductors [3–5], show temperature-dependent B_{1g} Raman spectra that are both remarkably similar and quite anomalous (see figure 1). This experimental material independence suggests that there is "universality" governing the electronic transport in correlated insulators. As these materials are cooled, they all show a reduction of low-frequency spectral weight with a simultaneous increase in the spectral weight of the high energy "charge-transfer" peak. This spectral weight transfer is slow at high temperatures and then rapidly increases as the temperature is lowered past an onset temperature that is in the proximity of the quantum-critical point corresponding to a metal–insulator transition. The Raman spectral range is also separated into two regions: one, where the response decreases as T is lowered and one, where the response increases. The characteristic frequency that divides these two regions is called the isosbestic point, which is the frequency where the Raman response is independent of temperature. Finally, if we view the Raman spectral gap as a measure of the insulating gap Δ that occurs at low temperature, and the onset temperature, where the weight initially is reduced, as a "transition temperature" T_c, then $2\Delta/k_B T_c$ is much larger than the weak-coupling value of 3.5. These anomalous features are not typically seen in either the A_{1g} or the B_{2g} channels.

Experimental results are plotted in figure 1. The top panel shows SmB_6, which has the added feature of developing a sharp peak at 130 cm^{-1} (that does not disperse in frequency) when the temperature is lower than 30 K. The FeSi data is shown in the middle panel. It displays the cleanest signature of these anomalous features. Note how the isosbestic point only develops at temperatures below 150 K. The bottom panel shows smoothed data in the LSCO high-temperature superconductor. The isosbestic point is somewhat harder to see here (because of the noise in the data), but it does develop at about 2100 cm^{-1} as the temperature is lowered.

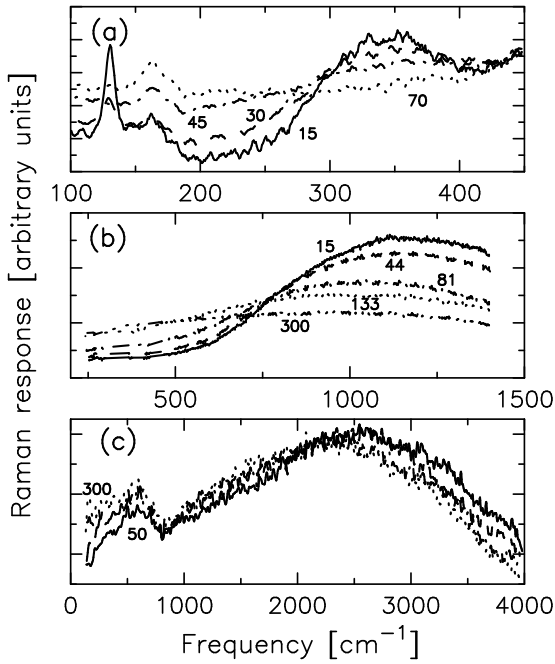

Fig. 1. Experimental B_{1g} Raman response for correlated materials (a) SmB_6 [1]; (b) FeSi [2]; and (c) underdoped $La_{2-x}Sr_xCuO_4$ [3] with $x = 0.08$. All of the experimental data show the development of a low-temperature isosbestic point, which occurs due to the transfer of spectral weight from low energy to high energy as the temperature is lowered, indicating the proximity to the quantum-critical point of a metal–insulator transition. The individual curves are labeled by the temperature in K where the measurement was taken. In panel (c) only the high temperature (300 K) and the low temperature (50 K) curves are labelled. The two intermediate curves are at 100 and 200 K, respectively.

Theory has lagged behind experiment for electronic Raman scattering in strongly correlated materials. While theories that describe Raman scattering in weakly correlated (Fermi-liquid) metals [6] or in band insulators [7] have been known for some time, it is only recently that a theory that describes materials near the metal–insulator transition has been developed [8,9]. This theoretical treatment involves applying the dynamical mean-field theory to two many-body systems that have quantum-critical points — the spinless Falicov–Kimball model [10] and the Hubbard model [11]. The Falicov–Kimball model is chosen, because it is the simplest model that displays these anomalies on the insulating side of the metal–insulator transition. The Hubbard model is chosen because it is the simplest model that has a metal–

insulator transition from a Fermi-liquid metallic phase. While qualitative results are model-independent on the insulating side of the transition, the Fermi-liquid behavior produces a number of new features that have not yet been seen in experiment.

The nonresonant B_{1g} Raman response is determined by the frequency-dependent charge susceptibility, with form factors associated with the corresponding symmetry channel appearing at the electron–photon vertices. Since the B_{1g} form factor is orthogonal to the lattice, there are no many-body vertex corrections [8, 12, 13], since the dynamical charge vertex has A_{1g} symmetry. Hence, the B_{1g} Raman response is represented by the bare bubble. Explicitly calculating the Raman response yields

$$\mathrm{Im}R(\nu) = c \int d\omega \{f(\omega) - f(\omega+\nu)\} \int d\varepsilon \rho(\varepsilon) A(\varepsilon,\omega) A(\varepsilon,\omega+\nu)\,, \qquad (1)$$

where $f(\omega) = 1/\{1+\exp(\omega/T)\}$ is the Fermi function,

$$A(\varepsilon,\omega) = \mathrm{Im}(-1/\pi\{\omega+\mu-\Sigma(\omega)-\varepsilon\})$$

is the spectral function, $\rho(\varepsilon)$ is the noninteracting density of states (a Gaussian here), and c is a constant. Hence the Shastry–Shraiman relation [14] holds — the nonresonant B_{1g} Raman response is proportional to the optical conductivity divided by the frequency. We use dynamical mean-field theory on a hypercubic lattice to calculate the many-body Green's functions. Once they are determined on the real axis, substitution into Eq. (1) yields the Raman response.

2. Results for the Falicov–Kimball model

The Falicov–Kimball Hamiltonian contains two types of electrons: itinerant band electrons and localized (d or f) electrons. The band electrons can hop between nearest neighbors (with hopping integral $t^*/(2\sqrt{d})$ on a d-dimensional cubic lattice [15]), and they interact via a screened Coulomb interaction with the localized electrons (that is described by an interaction strength U between electrons that are located at the same lattice site). All energies are measured in units of t^*. The Hamiltonian is

$$H = -\frac{t^*}{2\sqrt{d}} \sum_{\langle i,j\rangle} d_i^\dagger d_j + E_f \sum_i w_i - \mu \sum_i (d_i^\dagger d_i + w_i) + U \sum_i d_i^\dagger d_i w_i\,, \qquad (2)$$

where $d_i^\dagger$ (d_i) is the spinless conduction electron creation (annihilation) operator at lattice site i and $w_i = 0$ or 1 is a classical variable corresponding to the localized f-electron number at site i. We will adjust both E_f and μ

so that the average filling of the d-electrons is $1/2$ and the average filling of the f-electrons is $1/2$ ($\mu = U/2$ and $E_f = 0$).

The Falicov–Kimball model has a ground state that is not a Fermi liquid because the lifetime of a quasiparticle is finite at the Fermi energy. In addition, the imaginary part of the self energy has the wrong sign of curvature to be a Fermi liquid. As U increases, the system first enters a pseudogap phase, where spectral weight is depleted near the chemical potential, and then undergoes a metal–insulator transition (the pseudogap phase is possible because the ground state is not a Fermi liquid). The interacting Density Of States (DOS) is, however, temperature-independent for fixed U and fixed electron fillings [16]. It is plotted in Fig. 2 for a range of values of U: $U < 0.65$ corresponds to a weakly-correlated metal, while a pseudogap phase appears for $0.65 < U < 1.5$ moving through a quantum critical point at $U = 1.5$ to the insulator phase $U > 1.5$ (we neglect all possible charge-density-wave phases here).

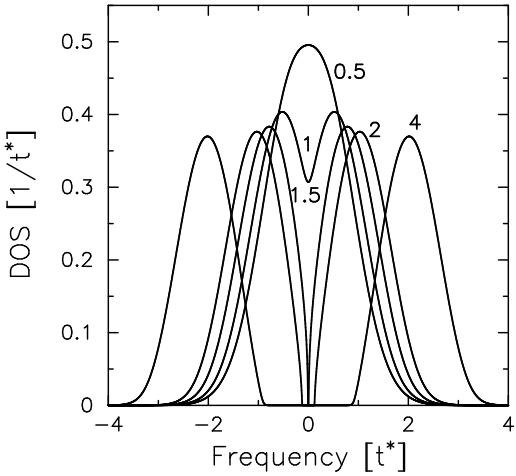

Fig. 2. Interacting density of states for the Falicov–Kimball model. Results are shown for $U = 0.5$, 1, 1.5, 2, and 4 (the numbers in the figure label the value of U). Note how the system first develops a pseudogap (1.0) before the metal–insulator transition at $U = 1.5$. The density of states is independent of temperature for the infinite-dimensional Falicov–Kimball model.

In figure 3 we plot the nonresonant B_{1g} Raman response at a fixed temperature $T = 0.5$ for different values of U. For small values of U, a small scattering intensity is observed due to the weak interaction among "quasiparticles" providing a small region of phase space allowable for pair scattering. The peak of the response reflects the dominant energy scale for scattering, as is well known in metals [6] and the high-energy tail is the cutoff deter-

mined by the finite energy band. This shape is also understandable from the Shastry–Shraiman relation — since the optical conductivity is a Lorentzian, the Raman response is just proportional to $a\nu/(\nu^2 + a^2)$, which assumes the above form. As U increases, the low-frequency response is depleted as spectral weight gets shifted into a large charge transfer peak at a frequency $\sim U$. The charge transfer peak begins to appear for values of U for which the DOS is still finite at the Fermi level ($U = 1$) and becomes large in this pseudogap phase before growing even larger in the insulating phase. Notice how low-frequency spectral weight remains even as one is well on the insulating side of the quantum critical point ($U = 4$) and at a temperature T much lower than the insulating gap. It is these spectral features that are characteristically seen in the experiments and which can only be seen in a theory that approaches the quantum critical point.

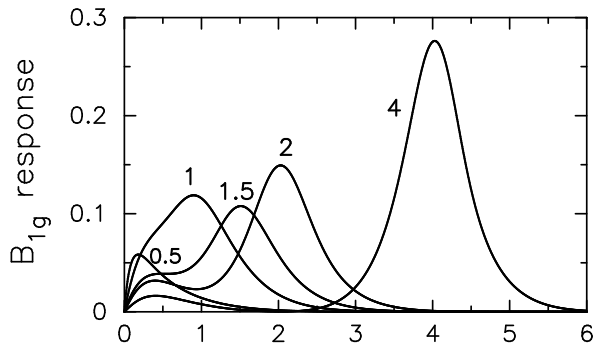

Fig. 3. Nonresonant B_{1g} Raman response for different values of U at $T = 0.5$. The Raman response is measured in arbitrary units. Notice how a low-energy peak and a charge-transfer peak (centered at U) separate from each other as the correlations increase through the metal–insulator transition.

Since the Raman response displays anomalous features on the insulating side of the metal–insulator transition, we present results for $U = 2$, just on the insulating side of the quantum critical point. In figure 4, we plot the temperature dependence. The total spectral weight increases dramatically with decreasing temperature as charge transfer processes become more sharply defined. At the same time, the low-frequency response depletes with lowering temperatures, vanishing at a temperature which is on the order of the $T = 0$ insulating gap (we are unable to analytically estimate the crossover temperature). This behavior is precisely what is seen in experiments on [2] FeSi and on [3] underdoped $La_{2-x}Sr_xCuO_4$ at low temperatures, where both the isosbestic point and the low temperature spectral weight depletion can be seen. Similar results are also seen [1] in SmB_6, but a low-energy peak also develops in that material at low temperatures.

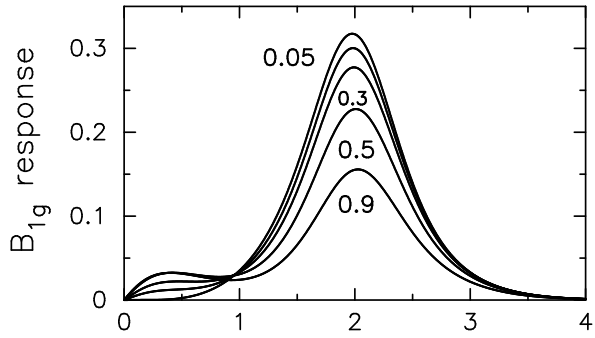

Fig. 4. Nonresonant B_{1g} Raman response for a range of temperatures ($T = 0.05, 0.2, 0.3, 0.5, 0.9$) for $U = 2$ (which lies just on the insulating side of the metal–insulator transition). The lines are labeled by their temperature (except for $T = 0.2$ which is unlabeled). Note how the B_{1g} response has low-frequency spectral weight that develops rapidly at an onset temperature of $T \approx 0.2$ (the low frequency response at T=0.5 and T=0.9 overlap) and note the isosbestic point at $\nu \approx 1$. The ratio of twice the range in frequency over which the low-frequency weight increases and the onset temperature is about 10.

If one were to interpret the temperature at which the B_{1g} Raman spectral weight starts to deplete as the "transition temperature" T_c and the range of frequency over which the weight is depleted as the gap Δ, then one would conclude that near the quantum critical point $2\Delta/k_B T_c \gg 1$. This is because the "T_c" is effectively determined by the gap in the single-particle DOS (which is small near the quantum critical point), while the "Δ" is determined by the width of the lower Hubbard band (which remains finite at the quantum critical point); hence the ratio can become very large near the quantum critical point (and should decrease in the large-U limit).

One can see from these results that all of the qualitative behavior common to correlated insulators is seen in the exact solution for Raman scattering in the Falicov–Kimball model — we see *(i)* the transfer of spectral weight from low energy to high energy as T is lowered; *(ii)* the development of an isosbestic point; and *(iii)* the ratio of twice the spectral range to the onset temperature where the low-energy spectral weight starts to deplete is much larger than 3.5.

3. Results for the Hubbard model

The Hubbard Hamiltonian [11] contains two terms: the electrons can hop between nearest neighbors (with hopping integral $t^*/(2\sqrt{d})$ on a d-dimensional hypercubic lattice [15]), and they interact via a screened Coulomb interaction U when they sit on the same site. All energies are measured in units of t^*. The Hamiltonian is

$$H = -\frac{t^*}{2\sqrt{d}} \sum_{\langle i,j\rangle,\sigma} c^\dagger_{i\sigma} c_{j\sigma} + U \sum_i n_{i\uparrow} n_{i\downarrow}\,, \tag{3}$$

where $c^\dagger_{i\sigma}$ ($c_{i\sigma}$) is the creation (annihilation) operator for an electron at lattice site i with spin σ and $n_{i\sigma} = c^\dagger_{i\sigma} c_{i\sigma}$ is the electron number operator. We adjust a chemical potential μ to fix the average filling of the electrons to half filling ($\mu = U/2$).

We study the evolution of the Raman response at half filling, since one can tune the system to move right through the quantum-critical point of the metal–insulator transition. We analyze finite-temperature numerical renormalization group calculations [17] (restricted to the paramagnetic phase which has a metal–insulator transition). We examine three cases here:

(i) a correlated insulator just above the transition $U = 4.24$ (where the response is model-independent);

(ii) a metal just below the phase transition $U = 3.54$ (which undergoes a temperature-dependent metal-insulator transition at $T \approx 0.011$); and

(iii) a correlated metal $U = 2.12$.

The Hubbard model DOS is temperature dependent, and we do not plot it here.

We show the correlated insulator regime in Fig. 5, where the Raman response is model-independent. We see behavior identical to that seen in the Falicov–Kimball model (the only modification here is the consequence of a temperature dependence in the interacting DOS, which fills in the gap at temperatures above about 0.1). We see the development of low-energy spectral weight at the expense of the higher-energy charge-transfer peak as T increases (although in this case the spectral weight grows over a broader temperature scale) and the appearance of a single isosbestic point at a somewhat higher energy than seen in the Falicov–Kimball model solution ($\nu \approx U/1.5$ rather than $\nu \approx U/2$). All of the qualitative features of the universal behavior are shared in the Hubbard-model solution. The difference is in the quantitative details, the most apparent one being that at high temperatures the low-energy spectral response does not have a broad peak structure, but

rather shows monotonic rising behavior. This is more characteristic of experiments in materials like FeSi [2] or the cuprates [3–5] which have a relatively flat low-energy spectral response.

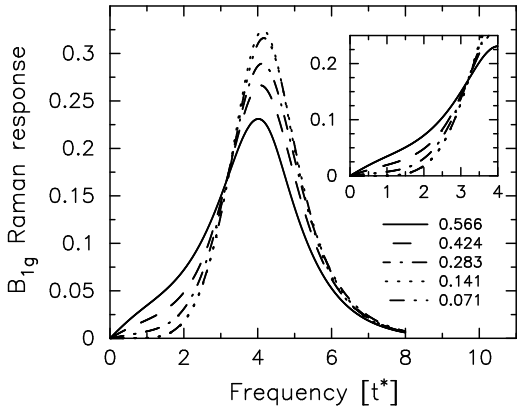

Fig. 5. Nonresonant B_{1g} Raman scattering for a correlated insulator $U = 4.24$ and half filling for a number of temperatures ranging from 0.57 to 0.071. Inset is an enlargement of the low-energy features.

In Fig. 6, we show results for a system tuned to lie just on the metallic side of the metal–insulator transition (so it undergoes a temperature-driven transition at $T \approx 0.011$). Initially the Raman response acts like an insu-

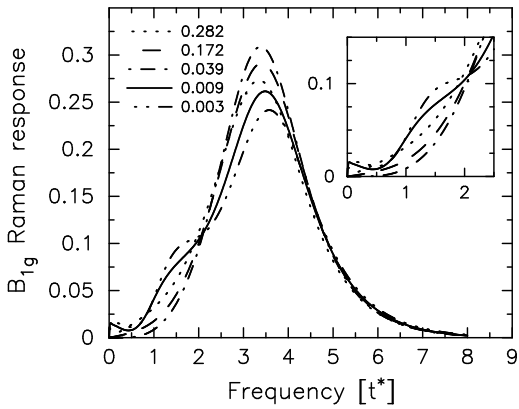

Fig. 6. Nonresonant B_{1g} Raman scattering for a system undergoing a temperature-driven metal–insulator transition $U = 3.54$ and half filling for a number of temperatures ranging from 0.28 to 0.003. Inset is an enlargement of the low-energy features.

lator: the charge-transfer peak sharpens and grows in strength, while the low-energy weight is reduced and an isosbestic point appears near $\nu = U/1.7$ as T is lowered. As the temperature is reduced further, the response becomes quite anomalous. Spectral weight shifts back out of the charge-transfer peak into the low-energy region, developing two low-energy bumps and an isosbestic point near $\nu = 2$. There is only one experimentally measured system that we know of that shares some of these qualitative features: SmB_6 [1]. At low temperatures SmB_6 acts like an insulator, just as seen in figure 6, but then at the lowest temperatures ($T < 30$ K), a sharp nondispersive peak appears at about 130 cm^{-1}. The qualitative shape of the Raman response is different though, because the weight only grows in a narrow peak, as opposed to the wide frequency range of figure 6. We believe it would be interesting to investigate the Raman response of a correlated system that undergoes a similar insulator–metal transition as a function of temperature such as 1% Chromium doped Vanadium Oxide [18]. Such experiments would be feasible if the charge-transfer peak could be pushed to a low enough energy that it lies within the window observable by Raman measurements.

Finally, in Fig. 7, we show the Raman response for a correlated metal at half filling. At high temperatures, the Raman response has a wide charge-transfer peak centered at $\nu \approx U$. As the temperature is lowered, we see the development and evolution of a low-energy Fermi-liquid peak, which sharpens as T is lowered. This is the classic behavior expected for a correlated metal — at high temperatures there is a large charge-transfer peak centered at an energy just somewhat higher than U which loses spectral weight as

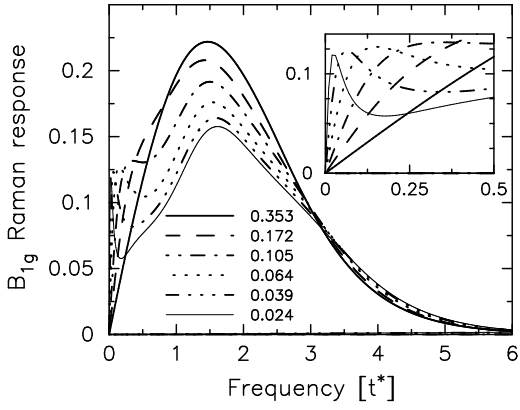

Fig. 7. Nonresonant B_{1g} Raman scattering for a correlated metal $U = 2.12$ at half filling for a number of temperatures ranging from 0.35 to 0.024. Inset is an enlargement of the low-energy features.

the temperature is lowered and a low-temperature "metallic" peak develops at low energy. The Fermi peak has the expected form proportional to $\nu T^2/[T_0(\nu^2+T^4/T_0^2)]$ for a Fermi liquid. The width of the peak (determined by T^2/T_0) decreases as the temperature is lowered and will ultimately vanish at $T=0$. The weight in the metallic peak is much smaller than the weight in the charge-transfer peak. The continuous evolution of the low-temperature peak down to zero frequency is not seen in the Falicov–Kimball model, because the self energy remains finite there in the limit as $T \to 0$. Note that the charge-transfer peak *loses* weight (especially on the low-frequency side) as T is lowered, but there is no low-energy isosbestic point here (in fact an isosbestic point may be developing at $\nu \approx 3.3$). This lack of low-energy isosbestic behavior is quite interesting. The development of a large-weight Fermi coherence peak in the interacting DOS tends to destroy the isosbestic behavior.

Unfortunately, we are not aware of any experimental data on a correlated metal that displays this low-temperature development and evolution of the Fermi-liquid peak. Surprisingly, little is known about Raman scattering in a weakly interacting metal. It is well known that in the absence of inelastic scattering, the low energy Raman cross-section vanishes at $q=0$ due to the lack of phase space available to create particle–hole pairs. Therefore, any signal at all must come from electron–electron interactions [19] or impurities [20]. Our results show that the consequence of well-defined quasiparticles is the presence of a low energy peak which grows in intensity and narrows as temperature decreases. Such a peak might also be observable in materials like $CeSi_2$, $CeSb_2$, $CeBe_{13}$ [21] or $YbAl_3$ [22] which all display the development of a low-temperature Fermi coherence peak at energies less than 100 meV.

4. Conclusions

To summarize, we have examined Raman scattering in correlated materials that fall into two classes — non-Fermi-liquid and Fermi liquid metallic states. We find in the insulating regime, the Raman response is model-independent, and illustrates all of the anomalies seen in experiment. In the metallic phase, there is interesting behavior when one has a Fermi liquid metal and one is close to the metal–insulator transition. Such systems are expected to have dramatic spectral weight shifts as a function of temperature as the system is tuned to pass through the metal–insulator transition. It would be interesting to see experimental work on these systems if the spectral weight shifts can be made visible within the spectral range accessible to Raman scattering experiments.

J.K.F. acknowledges support of the National Science Foundation under grant DMR-9973225. T.P.D. acknowledges support from the National Research and Engineering Council of Canada. R.B. acknowledges support by the Deutsche Forschungsgemeinschaft, through the Sonderforschungsbereich 484. We also acknowledge useful discussions with S.L. Cooper, R. Hackl, J.C. Irwin, M.V. Klein, and S. Shastry. We also thank S.L. Cooper, R. Hackl, and J.C. Irwin for sharing their data with us.

REFERENCES

[1] P. Nyhus, S.L. Cooper, Z. Fisk, J. Sarrao, *Phys. Rev.* **B52**, R14308 (1995); *Phys. Rev.* **55**, 12488 (1997).

[2] P. Nyhus, S.L. Cooper, Z. Fisk, *Phys. Rev.* **B51**, R15626 (1995).

[3] T. Katsufuji, Y. Tokura, S. Uchida, *Phys. Rev.* **B48**, 16131 (1993); X.K. Chen, J.G. Naeini, K.C. Hewitt, J.C. Irwin, R. Liang, W.N. Hardy, *Phys. Rev.* **B56**, R513 (1997); J.G. Naeini, X.K. Chen, J.C. Irwin, M. Okuya, T. Kimura, K. Kishio, *Phys. Rev.* **B59**, 9642 (1999).

[4] M. Opel, R. Nemetschek, C. Hoffmann, R. Philipp, P.F. Müller, R. Hackl, I. Tütto, A. Erb, B. Revaz, E. Walker, H. Berger, L. Forró, *Phys. Rev.* **B61**, 9752 (2000).

[5] M. Rübhausen, O.A. Hammerstein, A. Bock, U. Merkt, C.T. Rieck, P. Guptasarma, D.G. Hinks, M.V. Klein, *Phys. Rev. Lett.* **82**, 5349 (1999); S. Sugai, T. Hosokawa, *Phys. Rev. Lett.* **85**, 1112 (2000).

[6] To our knowledge no comprehensive review of electronic Raman scattering in metals exists. General ideas are covered in P.M. Platzmann, N. Tzoar, *Phys. Rev.* **136**, A11 (1964); A.A. Abrikosov, V.M. Genkin, *Zh. Eksp. Teor. Fiz.* **40**, 842 (1973) [*Sov. Phys. JETP* **38**, 417 (1974)]; A. Zawadowski, M. Cardona, *Phys. Rev.* **B42**, 10732 (1990); T.P. Devereaux, A.P. Kampf, *Phys. Rev.* **B59**, 6411 (1999).

[7] A.V. Chubukov, D.M. Frenkel, *Phys. Rev.* **B52**, 9760 (1995).

[8] J.K. Freericks, T.P. Devereaux, *J. Cond. Phys.* (Ukraine) **4**, 149 (2001); submitted to *Europhys. Lett.*, `cond-mat/0011013`.

[9] J.K. Freericks, T.P. Devereaux, R. Bulla, submitted to *Phys. Rev. Lett.*, `cond-mat/0104048`.

[10] L.M. Falicov, J.C. Kimball, *Phys. Rev. Lett.* **22**, 997 (1969).

[11] J.C. Hubbard, *Proc. Roy. Soc. London*, **A276**, 238 (1963).

[12] A. Khurana, *Phys. Rev. Lett.*, **64**, 1990 (1990).

[13] J.K. Freericks, T.P. Devereaux, to appear in *Phys. Rev.* **B**, `cond-mat/0104047`.

[14] B.S. Shastry, B.I. Shraiman, *Phys. Rev. Lett.* **65**, 1068 (1990); *Int. J. Mod. Phys.* **B5**, 365 (1991).

[15] W. Metzner, D. Vollhardt, *Phys. Rev. Lett.* **62**, 324 (1989).

[16] P.G.J. van Dongen, *Phys. Rev.* **B45**, 2267 (1992); P.G.J. van Dongen, C. Leinung, *Ann. Phys. (Leipzig)*, **6**, 45 (1997).

[17] R. Bulla, *Phys. Rev. Lett.* **83**, 136 (1999); R. Bulla, T.A. Costi, D. Vollhardt, *Phys. Rev.* **B64**, 045103 (2001).

[18] D.B. Mc Whan, A. Menth, J.P. Remeika, W. F. Brinkman, T.M. Rice, *Phys. Rev.* **B7**, 1920 (1973); G.A. Thomas, D.H. Raphine, S.A. Carter, A.J. Millis, T.F. Rosenbaum, P. Metcalf, J.M. Honig, *Phys. Rev. Lett.* **73**, 1529 (1994); M.J. Rozenberg, G. Kotliar, H. Kajueter, G.A. Thomas, D.H. Raphine, J.M. Honig, P. Metcalf, *Phys. Rev. Lett.* **75**, 105 (1995).

[19] A. Virosztek, J. Ruvalds, *Phys. Rev. Lett.* **67**, 1657 (1991); T.P. Devereaux, A.P. Kampf, *Phys. Rev.* **B59**, 6411 (1999).

[20] A. Zawadowski, M. Cardona, *Phys. Rev.* **B42**, 10732 (1990).

[21] J.J. Joyce, A.J. Arko, J. Lawrence, P.C. Canfield, Z. Fisk, R.J. Bartlett, J.D. Thompson, *Phys. Rev. Lett.* **68**, 236 (1992).

[22] L.H. Tjeng, S.-J. Oh, E.-J. Cho, H.-J. Lin, C.T. Chen, G.-H. Gweon, J.-H. Park, J.W. Allen, T. Suzuki, M.S. Makivic, D.L. Cox, *Phys. Rev. Lett.* **71**, 1419 (1993).